1980

Giant multipole resonances in the deformed fissionable nucleus 238U: breakdown of the hydrodynamical models?

Pitthan, R.

Monterey, California. Naval Postgraduate School

NAVAL POSTGRADUATE SCHOOL

Monterey, California

GIANT MULTIPOLE RESONANCES IN THE DEFORMED FISSIONABLE NUCLEUS ^{238}U: BREAKDOWN OF THE HYDRODYNAMICAL MODELS?

R. Pitthan, F.R. Buskirk, W.A. Houk,
and R.W. Moore
Department of Physics and Chemistry

Abstract

The deformed, fissionable nucleus ^{238}U was studied with inelastic scattering of 87.5 MeV electrons between 5 and 40 MeV excitation energy with inelastic momentum transfers ranging from 0.32 fm^{-1} to 0.58 fm^{-1} for an excitation energy of 15 MeV. Resonance cross sections extracted were compared with DWBA calculations using the Goldhaber-Teller, Steinwedel-Jensen, and Myers-Swiatecki models of the giant resonance. It is demonstrated that up to the first minimum of the form-factor the cross section is nearly completely determined by one parameter, the transition radius R_{tr}.

Using the known systematics of various multipole resonances in other, non-fissionable, nuclei as a guide, it was found that the assumed ground state radius of ^{238}U had to be enlarged by about 10% for all multipolarities, to bring the strength found in agreement with the systematics and with other experiments in ^{238}U. In particular, while the model-independent values for position and width of the GDR agree well with photon experiments, a scaled version of the Myers-Swiatecki model had to be used to produce agreement in strength. Similarly a scaled Goldhaber-Teller model was used for the isoscalar E2 resonance at 9.9 MeV. The situation for the isovector states above the GDR, E2 and E3 (or E0) is even more complicated. It is argued that with proper caution and consideration of other available data the use of the collective models mentioned above may give valuable insight into the charge distribution of ^{238}U at higher excitation energies.

I. Introduction

In recent years, there has been a renewed interest in the structure of the nuclear continuum. This interest has been stimulated by the discovery of numerous electric and magnetic isoscalar and isovector resonances of various multipolarity above particle threshold (giant resonance) which had been predicted a long time ago by Bohr and Mottelson[1].

Most of the experiments were done with inelastic scattering concentrating on the isoscalar quadrupole state (GQR) at 63 $A^{-1/3}$ MeV, whereby the analysis was based on macroscopic models[2-5]. The macroscopic models have contributed very much to our understanding of the nucleus because they allow one to describe the dynamics of a complicated many-body system in a simple way[6,7]. The use of the same concept in evaluating data taken with different probes and at different laboratories has made possible comparison of the results, mostly expressed in terms of a 'model-independent' sum rule, which has been very fruitful for the progress of the field[8]. It should be emphasized, however, that although the sum rule depends only on the nuclear ground state charge distribution and is indeed nearly model-independent, the amount exhausted by a certain resonance depends critically on the model used. Another important point is that in the momentum transfer covered by most (e,e') experiments, which rarely went beyond the first minimum in the formfactor, the momentum transfer dependence of the cross section is completely determined by just one parameter, the transition

radius $R_{tr}^{\lambda} = [<r^{\lambda+2}>/<r^2>]^{1/2}$, as will be shown below, quite similar to the description of the elastic cross section at low momentum transfer by the ground state rms-radius.

Since the GDR fragments in a spectacular way into separate oscillations along long and short axis'[9,10], immediately after the discovery of GQR's as systematic features of heavy nuclei interest focused onto the question whether or not this mode of excitation would fragment correspondingly.

These experiments are complicated, because due to the splitting of the GDR, its lower branch and the isoscalar E2 can no longer be separated by line shape, since they fall on top of each other. Certain assumptions for the form-factor of the GDR have, therefore, to be made in order to subtract it from the total cross section measured.

To do so, extensions of the Goldhaber-Teller model have been used in the past for the GDR, by introducing different spherical transition charge densitites for the dipole oscillations along long (R_z, $K = 0^-$) and short ($R_\perp$, $K = 1^-$) axis'[11], based on scaling the half density radius of the hypothetical ground state charge distribution, which enters the formulas of the hydrodynamic models, in the ratio of long and short axis, respectively, to the average radius[12,13,14]. This approach has been critized by Suzuki and Rowe[15], who showed that the scaling assumption is only valid for the $K = 1^-$ branch of the GDR. Since the $K = 0^-$ branch is the one which is lower in excitation energy, thus nearly

completely overlapping the GQR, a quantitative re-analysis seems to be in order. Fortunately, it turns out that the quantitative changes are relatively small, at least compared to the changes due to the use of different models of the giant dipole resonance.

To conclude the introduction we would like to quote from the conclusion of an unpublished report[16], which evaluated the data taken in Monterey on ^{238}U with a strict, that is not modified in any way, Goldhaber-Teller model. One of the salient points in this report was the surprisingly low E2 strength, comprising only 40% of the E2 sum rule for both isoscalar and isovector state:

> "The low E2 strength leads to the question whether the strict hydrodynamical model which has been successful in describing the data in non-fissionable nuclei can also be applied to ^{238}U for quadrupole excitations, or if the quadrupole strength is shifted to lower energy or spread out in a non-resonant way. Although this problem will need more experimental work, one may reason that for a fissionable nucleus the rms-radius for the charge distribution in the excited state may be expected to be greater than the one calculated from the hydrodynamical model.. ... such an assumption leads to a greater sum rule exhaustion, but still does not explain why this effect should be very strong for E2 oscillations, but not noticeable for E1 excitations".

In fact, it will become apparent below that what this problem needs is more theoretical consideration, and that there is a set of parameters which allows a consistent description of giant resonances in ^{238}U, consistent what concerns results from lighter nuclei as well as a comparison of different multipolarities in ^{238}U itself.

II. Previous Experiments with ^{238}U

In recent years, the giant dipole resonance has been extensively studied with various photon techniques.

Bar-noy and Moreh[17] utilized thermal neutron capture, Gurevich, et al.[18,19], employed Bremsstrahlung beams, and Veyssière, et al.[20], and Caldwell[21], et al., used quasi-monochromatic photons. The four above research groups located the maxima of the two branches of the giant dipole resonance in ^{238}U at excitation energies of about 10.9 and 14.0 MeV.

There is also work on the giant quadrupole resonance. With proton scattering a "bumplike" resonance was found by Lewis and Horen in the 10-13 MeV excitation energy range which was interpreted as a quadrupole resonance[22]. Approximately 85% of the isoscalar sum rule was exhausted. Wolynec, Martins, and Moscati[23] have used the (e,α) reaction to investigate the giant quadrupole resonance. Eighty-five percent of the isoscalar energy weighted sum rule (EWSR) was exhausted by a Breit-Wigner shaped resonance centered at 8.9 MeV with width Γ = 3.7 MeV. Since the α-decay probability at such low excitation energy is expected to be very small due to inhibition by the Coulomb barrier, while there are many open channels for both fission and neutron decay, the experiment of ref. 23 has been subject to scrutiny. All these experiments[24,25] agree in that the reported (e,α)cross sections are in error.

More constructively, several groups have searched with electrofission methods for E2 strength in ^{238}U. Shotter et al.[26], measuring the fission products, concluded that the asymetric component was due to the GDR, and therefore, to E1 absorption, while the symmetric component possibly could be due to an E2 component. Lack of accurate E2 virtual photon calculations for heavy nuclei prevented these authors from more definite conclusions.*) Kneissl et al.[27], had to include E2 cross section with a height of 40 mb at 22 MeV to explain a shoulder in their cross section. If one assumes this E2 strength to be concentrated in a 5 MeV wide resonance, it would result in approximately 130% of the EWSR ($\Delta T = 1$, E2), a somewhat high but still reasonable value. Since their spectra go only down to 10 MeV no investigation of the isoscalar resonance was possible. Most recently Arruda Neto et al.[28], found a GQR at 9.9 MeV with a width of 6.8 $\pm$ 0.4 MeV, exhausting 71% of the EWSR. Their data, in addition, are compatible with an M1 resonance centered at 6.5 MeV with a spreading width of 1.5 MeV.

---

*) Note added in proof

In a later experiment however, Shotter et al. concluded that E2 strength around 10 MeV was needed to give a fit to the electro fission 26a and electro neutron 26b data, but assuming only an E2 resonance at 22 MeV explained the data nearly as well. Since presumably both are present, their quantitative results may change somewhat, but it is unclear how much the value of Γ_n/Γ_f for the E2 component, they deduced to be 0.3 to 0.6, will change.

III. Present Experiment

The present experiments were undertaken to measure the excitation energies, width and cross sections of discernable resonances of a deformed dissionable nucleus by inelastic electron scattering. Samples of 99.9% enriched ^{238}U were obtained from Ventron Corporation and rolled to 0.004 inches for scattering at 90°, 0.002 inches for the 60° and 75° scattering angles, and 0.001 inches for the 45°. Using three different target thicknesses made it possible to optimize count rates as compared to the radiative background while achieving the required statistical accuracy.

87.5 MeV electrons from the NPS 120 MeV electron LINAC were scattered by the self-supporting ^{238}U foils at the scattering angles mentioned above, thus using the variation of the momentum transfer with angle to investigate the multipolarity of the giant resonances. A wider spread of angles was not necessary because the maxima of E1 to E4 formfactors are inlcuded in this range (figure 1) and would also be very difficult to measure, because at forward angles the radiation tail becomes so dominant that the beam has to be reduced to several nA only; at backward angles the inelastic cross section became very small, a fact which is often overlooked due to the use of relative cross sections σ/σ_{Mott} in the analysis of the data. E.g., the cross section for the GDR falls of two orders of magnitude from 45° to 90° at 87.5 MeV.

The scattered electrons were detected by a counter ladder in the focal plane of a 16" magnetic spectrometer. The general set-up of the NPS linear accelerator has been recently described in more detail[29], the problems and techniques to deal with the experimental and radiative background can be found in ref. 30. For completeness, a short compilation of other pertinent information is given below.

IV. Evaluation

The techinques employed were similar to those used in earlier (e,e') experiments with ^{208}Pb, ^{197}Au, ^{165}Ho, ^{140}Ce and ^{89}Y (refs. 31,13,30,29) so that comparisons between the nuclei could be made without variations from differing methods of evaluation. The points where the evaluation had to differ will be stressed at the end of this section. Special difficulties arise in the case of ^{238}U for extraction of the cross sections because the radiation tail, which has a strength approximately proportional to Z^2, is extremely large (figure 2). Furthermore, because the nucleus is deformed, the resonances are possibly split, as has been observed for the dipole state, or at least broadened and tend to be more spread out than in spherical nuclei[12,13,14], thus resulting in a very unfavorable signal to background ratio.

On the other hand, though large, the radiative background in (e,e') is well understood and although no rigorous treatment is possible yet, due to practical improvements the calculations account for virtually all the radiative background[30]. It is especially to be noted that the two regions where one knows the background experimentally (namely between low-lying isolated levels and above 40 to 50 MeV excitation energy), are reproduced within a few percent in spherical nuclei[29,30].

Our evaluation is sensitive to resonant structure only; more continuous cross sections, e.g., from the tail of the quasi elastic peak, would not be seen with our method,

The inelastic cross sections were measured relative to the elastic ones. The latter, in turn, were calculated with a phase shift code[32] using the Fermi ground state charge distribution parameters c = 6.805 fm and t = 2.66 fm. These parameters, which are from elastic electron scattering, were taken from the compilation by De Jager, et al[33].

The inelastic spectra were evaluated using a least square line shape fitting program, as described recently[29] in which the resonances and the background are fit simultaneously. Since the elastic cross section σ_{el} can be calculated, and the areas under elastic peak and an inelastic resonance, A_{el} and A_{in}, follow the relation $\sigma_{el}/\sigma_{in} = A_{el}/A_{in}$, σ_{in} is determined by the inelastic area. To determine the latter, the background has to be subtracted. The largest portion of the total background is due to the elastic radiation tail which is caused by photon emission before, during and after the scattering event, plus energy straggling and ionization. The radiation tail was calculated using the Born approximation formulas of Ginsberg and Pratt but substituting the actual elastic cross section at the energy of the scattered electron, computed with the phase shift code of Fischer and Rawitscher[32].

In addition to the radiation tail, the experimental background, consisting of general room background and of electrons scattered by the targets and subsequently rescattered by the spectrometer walls, had to be taken into account. The total background was found to be well described with a three

parameter function:

$$BGR(E_f) = P_1 + P_2/E_f + P_3\, T_R(E_f)$$

or

$$BGR(E_f) = P_1 + P_2\,(E_f - E') + P_3\, T_R(E_f),$$

where the P_i are fitting parameters, E_f is the energy of the outgoing electron, E' is the center energy of the fitting range, and T_R is the radiation tail. The parameter P_3 turned out to be close to one which shows that little scaling of the calculated radiation tail was necessary, P_2 was small; otherwise the two functions could not have served equally well in describing the background because this term is the one different in both forms. No difference between the results obtained using the above two background functions was observed. The second function was used in the final analysis of all spectra. In addition, a bump from instrumental scattering (ghost peak) at 6.5 MeV had to be subtracted. The whole procedure has been thoroughly described in ref. 30.

It is quite evident from figure 2, that a fit which attempts to let the χ^2 method work its way to a minimum all by itself is not possible. Reasonable good starting values for background and resonances have first to be found, and constraints have to be put on some of the three resonance parameters position, height and width. While as a matter of principle, the height always was left variable, position and width of most resonances were fixed in any one computer run, but the free fitted ones were rotated.

Three alternate criteria have been generally used for assuming the presence of a resonance in the spectrum in the first place: (1) the observation of the resonance peaking above the flat expanse of the radiation tail and background, (2) the knowledge of resonances found by photonuclear and photofission experiments, (3) the necessity to add a resonance to achieve a consistent overall fit. In the case of uranium, it is difficult to use the first criterion for reasonable placement. As can be seen in the inelastic spectrum for 75° (figure 2), very few of the collective states are visible to the naked eye. It is only after the subtraction of the radiation tail and continuous spectrum due to Bremsstrahlung that the spectrum begins to exhibit the structure of the giant multipole resonances (figure 3).

The line shape used throughout was Breit-Wigner. This choice is based on the observation that the strength function, but not the cross section, for the GDR is best described by this form[35]. However, use of Lorentz form gives only slightly different resonance parameters, except for 0.2 - 0.5 MeV shift in excitation energy, which depends on excitation energy and multipolarity. We want to emphasize that all parameters given are those of the strength function, which is the only invariable, and not those of the cross section, which may be different for different experiments and probes[35].

As pointed out in the beginning, the reduced transition strength for giant resonances is often expressed as fractions

of the electromagnetic sum rules. This is particularly appropriate for electron scattering, because here the sum rules depend only on the nuclear charge distribution of the ground state (for a discussion of inherent difficulties in the case of hadronic probes, see ref. 36). In this paper the sum rule for $\lambda > 1$

$$S(E\lambda) = \frac{Z\,\lambda(\lambda+1)^2\hbar^2}{8\pi\,M_p} \langle R^{2\lambda-2}\rangle$$

was used, where M_p is the mass of the proton and $\langle R^{2\lambda-2}\rangle$ the $(2\lambda-2)$ - moment of the ground state charge distribution of the nucleus[37,38]. As to the distribution of strength between isoscalar and isovector parts, a fraction of Z/A was thought to be isoscalar, and the remainder, N/A, to be isovector[38]. This sum rule does not account for interference terms between isoscalar and isovector excitations, an assumption which is not true for N > Z nuclei[39], and may even be invalid for N = Z nuclei as light as ^{28}Si when due to the Coulomb force isospin is no longer a good quantum number. One should, therefore, regard the use of sum rules only as a generally accepted convenient measure for strength. Isoscalar and isovector sums in this simplified picture are thus related by

$$S(E\lambda,\ \Delta T = 1) = S(E\lambda,\ \Delta T = 0)(N/Z).$$

The energy-weighted isovector sum rule for the electric dipole resonance has to be modified because the center of

mass motion has to be zero[40]:

$$S(El) = \frac{9}{8\pi}\frac{\hbar^2}{M_p}(NZ/A) .$$

In the monopole case (breathing mode) the requirement of volume conservation leads to the equation[41]

$$S(E0) = \frac{\hbar^2}{M_p} A \langle r^2 \rangle .$$

The energy-weighted sum rules for ^{238}U, calculated with $\langle R^2 \rangle^{\frac{1}{2}} = 5.730$ fm and $\langle R^4 \rangle^{\frac{1}{4}} = 6.124$ fm, which in turn were calculated by numerical integration of the ground state charge distribution, are

$S(E0) = 3.24 \cdot 10^5$ MeV fm^2; $S(E2) = 2.49 \cdot 10^5$ MeV fm^4;
$S(E3) = 3.15 \cdot 10^7$ MeV fm^6; and $S(El, \Delta T = 1) = 839$ MeV fm^2.

The inelastic cross section is mostly presented in units of the Mott cross section

$$(d\sigma/d\Omega)_{Mott} = (\alpha Z/2Ei)^2 \cos^2(\theta/2)/\sin^4(\theta/2),$$

which describes the elastic scattering of an electron from an infinitely heavy, spinless, pointlike nucleus with charge Ze. Expressing the cross section in these units takes out most of the purely kinematical contributions, makes the nuclear contribution to the cross section more evident, and allows a convenient comparison with theoretical predictions. Through this comparison the determination of multipolarities and strength is made.

In the present work this determination is based on calculations using the distorted wave computer code of Tuan, et al.[42], which requires a model for the nuclear transition charge, current, and magnetization densities. For strongly collective transitions it has been found that it is sufficient to take into account the charge contribution only[43]. The problem then rests with the choice of model and the question whether or not the ground state charge distribution, $\rho_o(r)$, which enters all collective models, has to be modified. No such changes have been found necessary up to now for giant resonances, which may be not too surprising, because the continuum excitations of nuclear matter are the hydrodynamical modes of the nucleus[44]. The attempt to fit the transition charge densities to the experimental data at higher momentum transfer ($q \gtrsim 0.8$ fm^{-1}) in the case of ^{181}Ta leads to transition charge densities which are more concentrated in the nuclear interior than those of the hydrodynamical model[45]. The transition strengths found with these densities are a factor of 2 to 3 smaller than those from either other (e,e') experiments[46] in ^{181}Ta or from comparable nuclei[8]. The deviation between DWBA calculations and experiment in ^{181}Ta is probably due to not accounting for higher multipole strength instead of a failure of the hydrodynamical model. Further support for the application of the strict hydrodynamic model to giant resonances comes from the generally good agreement in strength extracted from (e,e'), (γ,n) and inelastic hadron scattering. For ^{238}U the case seems

to be different as evidenced by the results of ref. 16. Figures 4 and 5 demonstrate for the quadrupole resonances how much the results for ^{238}U deviate from what one would expect from measurements at lower A.[8]

For our purpose a convenient parameterization has been introduced by Ziegler and Peterson[43], by defining a half-density thickness c_{tr} and skin thickness t_{tr}, which replace the parameters c_t and t in the two-parameter Fermi distribution

$$\rho_o = C^0 \ (1 + \exp \ (r - c/z))^{-1} \ ,$$

with $z = 4 \ t \ \ln 3$, for calculating the transition charge density. A parameterization $c_{tr}/c = 1.1$, $t_{tr}/t = 1$, e.g., would mean that the "hypothetical" ground state charge distribution half-density radius has been enlarged by 10% while keeping the surface thickness constant.

The cross sections calculated with the DWBA code are normalized to $B(E\lambda, E_x=0) = 1.0 \ fm^{2\lambda}$, so that the experimental transition probability is simply calculated by fitting the calculated curve to the measured points.

Figures 6, 7 and 8 show the importance of the correct choice of model as well as parameterization, for E1, E2 and E3 transition, respectively, because a 10% change in radial dependence may produce more than 50% change in height at the maximum of the calculated relative cross section.

Before we discuss in more detail figures 6, 7 and 8 we will elaborate somewhat on the models used. The Tassie model[46] is generally regarded as the classical hydrodynamical model. Its transition charge distribution is identical with the Goldhaber-Teller model[47],

$$\rho_{tr}(r) = C^{GT} \ r^{\lambda-1} \ d\rho_o(r)/dr \ ,$$

corresponding to the oscillation of a rigid proton volume versus a rigid neutron volume. The Steinwedel-Jensen model[48],

$$\rho_{tr}(r) = C^{SJ} \ j_\lambda(r \ k_\lambda/c) \ \rho_o(r) \ ,$$

corresponds to the assumption of two interpenetrating proton and neutron liquids within one surface.

It has been difficult to determine experimentally which of these models is correct, since photon absorption measurements, the most exact method, is practically model-independent.

Only recently has experimental evidence in the form of the Myers-Swiatecki droplet model fits[49] been applied to this problem[50]. This approach resulted in a description of the GDR as a mixture of both GT and SJ modes

$$\rho^{MS}_{tr}(r) = C^{MS} \ (\rho^{GT}_{tr}(r) + \alpha(A,\lambda) \ \rho^{SJ}_{tr}(r)) \ ,$$

with $\alpha(A,1)$ rising from approximately 0.5 for Ni to 0.9 for ^{238}U. This concept has been also applied by Kodama[51] to higher isovector multipoles resulting in $\alpha = 0.5$ while $\alpha = 0$ is expected for isoscalar states. Recent experiments in

^{140}Ce (refs. 30,52) have shown that the data are well described by the predictions $\alpha(140, 1) = 0.65$ (ref. 50) and are compatible with $\alpha(140, 2) = 0.5$ (ref. 51).

Figure 6 shows several DWBA calculations for the GDR in ^{238}U in comparison. Based on the experiments in ^{140}Ce we believe that the model of Myers, et al.[50], is the best available description for the dipole case and calculations for three parameters, $c_{tr}/c = 0.9$, 1.0 and 1.2, are shown. The skin thickness was not changed. There are several important points to make. In PWBA the variable displayed, σ/σ_{Mott}, is a true formfactor and can be written as

$$F^2(q) = \sigma/\sigma_{Mott} = \frac{4\pi}{Z^2}(2\lambda+1)\left|\int \rho_{tr}(r)\, j_\lambda(qr)\, r^2\, dr\right|^2 ,$$

$$q = \frac{1}{\hbar c}\left(E_i^2 + E_f^2 - 2E_f E_f \cos\theta\right)^{\frac{1}{2}} ,$$

E_i initial, E_f final electron energy. That means that the relative cross section F^2 is a function of q only and that it will display the typical pattern of a spherical Bessel function. In heavy nuclei, where the plane wave approximation no longer works, two things happen. First, the relative cross section, for convenience often still called formfactor, is a function of two of the three variables E_i, θ and q. Consequently, curves for the same q, but different E_i, will be different. Secondly, the minima are washed out, especially for the El the first minimum is barely

visible, and occur at lower q compared to PWBA. Another important point is that, despite all these changes, up to the first minimum, or what is left of it, the curves are nearly identical for calculations with the same initial energy E_i, but different transition charge densities, if the transition radius $R_{tr} = \langle r^{\lambda+2}\rangle_{tr}/\langle r^2\rangle_{tr}$ is equal. But it is also apparent that differences beyond the first minimum can be quite large. This can, for example, be seen from comparison between the MS model ($c_{tr}/c = 0.9$), $R_{tr} = 6.30$ fm, and the SJ model ($c_{tr}/c = 1$), $R_{tr} = 6.26$ fm. As one would expect from the general trend, the calculation with the lower R_{tr} results in the higher curve. This is understandable because, as mentioned above, the cross sections in the DWBA code are normalized to

$$B(E\lambda) = (2\lambda+1)\left|\int r^\lambda \rho_{tr}(r)\, r^2 dr\right|^2 = 1\ \text{fm}^{2\lambda}.$$

Since the integral will be larger when R_{tr} is larger, the curves have to be lower. A compilation of various models and parameterizations and the R_{tr} which go with them is given in Table 1. Figure 7 shows similar calculations for the quadrupole case, but with the emphasis on the GT model ($c_{tr}/c = 0.9$, 1.0, 1.1, and 1.2). Again, a calculation with the MS model ($c_{tr}/c = 1$) which yields a R_{tr} close to the GT case ($c_{tr}/c = 0.9$) is nearly identical with the latter.

Two features emerge as compared to the El calculations (figure 6): the differences in height between curves with the same parameters as in the El case is larger (and will be

even larger for higher multipolarities, see figure 8, and the first minima are less washed out. Figure 8 finally shows a set of calculations for an octupole transition.

The conclusion from the actual variation in the models, displayed in figures 6 to 8 is that the strength extracted from (e,e') may be quite model-dependent, but the multipolarity determined from the position of the first maximum of the formfactor is much less sensitive.

Nevertheless, for all practical purposes in the momentum transfer covered by this experiment, a GT calculation for an E2 with $c_{tr}/c = 0.9$ is undistinguishable from calculation for E3 with $c_{tr}/c = 1.2$. This has to be kept in mind below where we try to get a unified and consistent picture and description of giant resonances in ^{238}U.

The error assignment to giant resonance cross sections has been found difficult by most authors (see, e.g., ref. 53). Since many uncertainties enter in the background determination the purely statistical error from solving the error matrix in the χ^2 fit is mostly too small. The errors shown for the cross sections in this paper are estimated total errors, which came out to be approximately twice the statistical errors. The estimate was based on how the areas under the curves, positions, and width could be changed during the fits due to different choice of resonance parameters,

background, ghost peak subtraction, etc., while still maintaining $\chi^2 < 1.1$.

As may be seen from the figures the typical estimated uncertainty for a given peak area for one angle is 20 to 30%. All other experimental errors are very minor in comparison (elastic phase shift < 1/2%, charge accumulation < 0.1%, inelastic DWBA < 1%, etc.) and have been, therefore, neglected.

The main other uncertainty comes from the model dependence and concerns only the extracted strength. The values quoted can easily be changed by a factor of two by changing the model or its parameterization. The estimated error per resonance stemming from the measurement and its estimated error are, in contrast, only 10 to 15%.

The question as to the model dependence has no easy answer. But it does not even have to be answered, because the thrust of this paper, as may be deduced from the quote from ref. 16 in the beginning, rather is whether or not the charge distribution for the excited states is more extended than that of the ground state, and whether or not the sum rule values can be brought into agreement with the systematic expectations (figures 4 and 5) and other experiments, with reasonable changes of the models used.

V. Results

A. General

Figure 3 showed the spectra taken and evaluated for the present work after subtraction of total background including the ghost peak, which in our spectrometer occurs at 92% of the elastic energy, i.e., approximately 7 MeV excitation energy. The resonances required for the simultaneous fit of spectra and background are indicated.

Several features are apparent without a detailed quantitative analysis. We know from photon work the position of the two branches of the dipole state, 11 and 14 MeV. If we take these resonances as reference, it is immediately apparent from figure 1 that the resonances at 10 and 22 MeV are of higher multipolarity, presumably E2, because this energy position corresponds to the well-known 63 and 135 $A^{-1/3}$ MeV dependence for the isoscalar and isovector E2[8]. The state at 28 MeV rises faster with angle or momentum transfer and thus has to be of higher multipolarity. The excitation energy, compared in $A^{-1/3}$ MeV units, is lower than the resonance-like structure found in ^{208}Pb and ^{197}Au (ref. 31), but agrees with the data from ^{181}Ta (ref. 45) and ^{165}Ho (ref. 12). All these arguments assume that only <u>one</u> multipolarity contributes to each resonant structure.

The one feature of figure 3 which does not fit into the simple picture as inferred from figure 1 is the resonant cross section at 17 MeV because it appears only at 45°and 90°. However, a resonance shape was required at this excitation

energy to achieve a satisfactory χ^2 fit, i.e., $\chi^2 < 1.1$, at these angles.

B. The Giant Dipole Resonance

The splitting of the GDR in ^{238}U into two branches has been measured by $(\gamma,n) + (\gamma,f)$[18-21] and (γ,γ') measurements[17]. The values for position and width agree well with our results (table 2), which can be taken from the fit to the spectra without much model dependence. Getting the strength (reduced transition probability $B(E\lambda)$, sometimes called B-value), is more involved.

In the Danos-Okamoto model of the GDR the splitting in deformed nuclei is interpreted as being due to difference in the resonant energies of oscillations directed along the longer and shorter radii, R_z and $R_\perp$, of the nuclear spheroid[9,10]. As outlined in the introduction, these oscillations are treated separately. The model parameters, R_z and $R_\perp$, are determined in the framework of the Danos-Okamoto model from the giant dipole energies, E_z and $E_\perp$. If we assume a uniform density within the spheroid we get a volume constraint

$$R_{eq}^3 = \frac{5}{3} \langle r^2 \rangle^{3/2} = R_z \cdot R_\perp^2,$$

where R_{eq} is the equivalent radius of a sphere. The Danos-Okamoto equation

$$R_z/R_\perp = (E_\perp/E_z - 0.089)/0.911$$

then enables the calculation of c_{tr}, yielding $c_{tr}^z = 1.24 \cdot c$

and $c_{tr}^{\perp} = 0.90 \cdot c$, assuming constant skin thickness. If one uses an unmodified, or 'strict', Goldhaber-Teller model for all resonances, the GDR is the only one for which reasonable values, or values in agreement with other experiments, concerning the sum rule are achievable. Figures 9 and 10 show a fit to DWBA calculations which were performed with the parameters of the strict GT model yielding B(El, long) = 28 fm^2 and B(El, short) = 49 fm^2, which agrees rather well with the γ results (table 2). In contrast, the MS model with c_{tr}/c = 1.24 and 0.9 does not do that well and would yield 23 and 37 fm^2, respectively. Since for the MS model values for both axis are smaller than the photon results (table 2), we have done the obvious and enlarged c_{tr} by approximately 10%, which brings c_{tr}/c to 1.0 and 1.36, respectively. Calculations using this value with the Myers-Swiatecki model are compared in figure 11 to the experimental data, resulting in B_{MS} (El, c_{tr}/c = 1.36, E_x = 11 MeV) = 50 fm^2 and B_{MS} (El, c_{tr}/c = 0.99, E_x = 14 MeV) = 30 fm^2. The strengths calculated with both models and both parameterizations are shown in table 2 together with the model independent γ results.

This is a rather confusing situation which seemingly does not lend itself to easy interpretation. However, the physical aspects simplify, if we look at table 1, and compare the transition radii for the different model and parameterization combinations which give similar strength values. One sees that R_{tr}(GT, 0.9) $\approx$ R_{tr}(MS, 1.0) and R_{tr}(GT, 1.24) $\approx$ R_{tr}(MS, 1.36) and consequently, due to the connection between R_{tr} and B(Eλ), the above result is no longer surprising.

It has been shown, that a large fraction of the El cross section[20,21] as well as the E2 cross section[28] is due to fission. Consequently, the enlargement of the ^{238}U nucleus in the giant resonance region should be less a function of multipolarity but of excitation energy. The above analysis will only appear reasonably sound if an analysis along these lines, ('blow-up' of the excited state charge distribution by approximately 10%) improves the agreement between results from other experiments and (e,e') in ^{238}U for <u>all</u> multipolarities. In the next subsection we will therefore, investigate the quadrupole states.

In summary, if one assumes the MS model to be the better choice (for arguments see, e.g., ref. 52), one has to conclude that the ^{238}U nucleus in the excited state is 10% larger than in the ground state.

C. <u>Isoscalar and Isovector Quadrupole Giant Resonance</u>

Besides the problem of the strength of the E2 states and its dependence on the model and parameterization used, as outlined earlier, the question of their widths is also of importance. Since it is not, or very little, model dependent it may serve as a measure for the reliability of an experiment. The width measured, or assumed, also influences the cross section under a resonance, especially in inelastic scattering where the background is fitted simultaneously with the resonances. Since the fits are most sensitive to the peak and its vicinity a width wrong by a factor of two would result in an area wrong by a factor of four, because the height,

that is the background base line, would also change by the same factor. The physical motivation for measuring the width of deformed nuclei has been given in the introduction.

There have been several calculations, both with microscopic and macroscopic theories, as to the width of the isoscalar quadrupole states in deformed nuclei. Comparison of ^{144}Sm and ^{154}Sm by Kishimoto, et al., showed a total theoretical splitting of 6 MeV for the K = 0, 1, 2 components while the experimental result from α-scattering was only 0.8 ± 0.3 MeV, namely from 3.9 MeV to 4.7 MeV for the broadening of the overall line shape[54]. Requiring self-consistency for the quadrupole-quadrupole interaction brought the total splitting down to 2 MeV, which results in a broadening in agreement with the experimental value. An (e,e') experiment in the same region of the nuclear system[12], ^{142}Nd compared to ^{152}Nd, showed a broadening of 2.2 MeV, namely from 2.8 ± 0.2 MeV to 5.0 ± 0.2 MeV, while (e,e') on ^{165}Ho showed Γ = 3.9 ± 0.4, which was compared to the GQR in ^{140}Ce and ^{208}Pb, both 2.8 MeV wide[13]. At the time references 13 and 54 were published, there was some mutual criticism on the results obtained by others; but this seems to have resolved by now[55].

Microscopic calculations using a quasiparticle RPA[56] predicted a broadening which varied appreciably in the three rare earth nuclei investigated (from 1.0 to 2.9 MeV, depending on the nucleus and assumption of the unperturbed line width), but no measurements have been done in these nuclei.

Macroscopic calculations based on a viscosity model by Auerbach and Yeverechyahu[57], by definition applicable to all A, give rough agreement with the general trend[8], but do not account for shell or deformation effects. An application of the theory of ref. 57 on deformed nuclei[58], shows qualitative agreement, as do more recent macroscopic calculations by Suzuki and Rowe[59]. The most detailed description of deformed nuclei has been published by Soloviev and coworkers[39,60] on the basis of Solovievs semi-microscopic model (for a more complete list of references to this work see ref. 61). Table 3 shows a comparison between this theory and experiment. In general, the agreement is good and shows the tendency of the width to decrease with increasing mass, expected from simple macroscopic considerations[57], but also shows individual variations from nucleus to nucleus as expected from a microscopic theory[56].

The next figures (12-14) shows that the resonances at 9.9 ± 0.2 MeV with a width of $2.9 \begin{smallmatrix} + 0.8 \\ - 0.4 \end{smallmatrix}$ MeV and at 21.6 ± 0.7 MeV with a width of 5.0 ± 0.6 MeV conform to a momentum transfer predicted by DWBA calculations for E2. Figures 4 and 5 had shown that the application of the 'strict' Goldhaber-Teller model lead to sum rule fractions which were lower than expected from other nuclei. Figures 12 and 13 show that despite that low strength the resonances conform to a E2 DWBA calculation.

To test our hypothesis that ^{238}U at higher excitation energy is more extended than in the ground state, we have

performed calculations analogue to the dipole case. Figure 14 shows a fit of DWBA calculations, based on the hydrodynamical models with a ground state change distribution scaled by 10%, to the experimental data. It is obvious that the fits are just as good as the ones in figure 12 and 13. Table 4 shows that, for the isoscalar state, the sum rule fraction of 77% is in reasonable agreement with other measurements though still lower than expected from figure 6. But this difference is meaningless in view of the strong model dependence.

There are no other direct measurements of the isovector E2 at 21.6 MeV. The only quantitative inference made, from the work of Kneissl, et al.[27], would lead to 130% of the EWSR (see section II), for which we estimate an error of 50% on the basis of the data of ref. 27. Our result, 70 to 88%, depending on the model used, has, as the other strengths given, a strong model dependence. As figure 14 shows this is mainly due to the fact that the data points are on the falling region of the formfactor. To overcome this difficulty data would have to be taken in the region of the second maximum, a difficult enterprise in itself due to the above mentioned rapid fall-off of the cross sections, and the increasingly strong excitation of higher multipoles as evident from figure 1.

The MS model calculation shown in figure 12 was based on $\alpha(238, 2) = 1.0$. Using $\alpha = 0.5$ from Kodamas work would raise the EWSR fraction from 70% to approximately 80%, but as one may infer from figure 14, not change the assignment

of E2 or any other conclusions.

It is somewhat dangerous to rely on the extrapolations from lower A in judging what might or might not be a reasonable value. But still, the strength has to be somewhere. So it either might be spread out through direct or semi-direct processes, or shifted to very low excitation energy. On the other hand, support for the hypothesis of assuming a 'blown-up' ^{238}U nucleus comes from the simultaneous improvement for both E1 and E2 states in comparison with results from other methods[18-21,27,28].

D. The State at 28 MeV

From figure 3 it is evident that the resonance-like structure, called resonance in the following, at 28.4 ($176\ A^{-1/3}$) MeV rises faster with momentum transfer than the E2 states at 10 and 22 MeV. In measurements in ^{140}Ce (ref. 30), ^{165}Ho (ref. 13), ^{181}Ta (ref. 45), and ^{197}Au and ^{208}Pb (ref. 31), a resonance at about the same excitation energy has been found, whereby a definite assignment proved difficult due to the high excitation energy which results in a large width and small peak cross section. Interpretation has been oscillating between E0 and E3 (ref. 8). Macroscopic predictions project the isovector E3 state[62] at around $190\ A^{-1/3}$ (30.5) MeV, and the isovector monopole[63] at $178\ A^{-1/3}$ (28.5) MeV. Microscopic calculations give compatible results (see, e.g., ref. 64).

Whatever it might be what has been seen at this high excitation energy, it was noted[8,30] that a resonance appeared at 195 $A^{-1/3}$ MeV in spherical nuclei but at ~180 $A^{-1/3}$ MeV in deformed nuclei.

It has, therefore, been speculated that the higher of the two resonances (if they are indeed of different multipolarity) might be E3, which fragments in a deformed potential and disappears in the background. The E0, on the other hand, is in spherical nuclei hidden between isovector E2 and E3 and becomes visible only in deformed nuclei. While decisive experiments still have to be performed, figure 15 shows that the data in ^{238}U are compatible with this explanation, because the cross section is large enough to accomodate 100% of the isovector monopole and 75% of the isovector octupole EWSR. For the E0 DWBA calculations of figure 15 the model by Schucan[65]

$$\rho_{tr}(r) = -3\rho_o(r) + d\rho_o(r)/dr$$

was used, which is identical with the one proposed by Satchler[66]. No model dependence was investigated for the monopole.

E. The Cross Section at 17 MeV

Figure 3 shows for the 45° and 90°, but not the 60° and 75° spectra, a resonance at 17 MeV. Since this behavior is somewhat at odds with the regular behavior predicted by figure 1 no definite answer as to the origin is possible. But this "resonance" was necessary to fit the spectra as outlined

earlier. If taken as a Breit-Wigner shaped state its excitation energy is $E_x = 17 \pm 2$ MeV and its width 3.9 ± 1.5 MeV. Although the resonance energy of 106 $A^{-1/3}$ MeV closely follows the isoscalar E3 resonance predicted by the self-consistent shell model[7,62], it does not follow the angular distribution for an E3 cross section. However, the momentum transfer found could be explained by a mixture of M1 and E3, because at 45° an M1 would be at the maximum of its form-factor. Since the measurements were not extended to sufficiently large or small angles to isolate transverse contributions no more definite statement can be made.

VI. Conclusions

We have investigated the giant resonance region of the fissionable, deformed nucleus ^{238}U with inelastic electron scattering. While other deformed nuclei have been investigated in the past, this experiment constitutes to our knowledge the first (e,e') measurement of a fissionable nucleus in the continuum. The difference to these other measurements is that the hydrodynamic models (GT for E2 and E3, and MS for the E1) apparently fail to describe the strength correctly.

Does that mean they break down and cannot and should not be used for the evaluation? It is clear from our paper that we concluded otherwise. As in other cases the collective models give an insight into the pheonomena of a complicated many body system that is difficult to achieve otherwise. In the present case it tells us that ^{238}U expands as it is excited to higher excitation energies. While it is tempting to refine the present analysis by investigating if the scaling factor c_{tr}/c is a function of the excitation energy, we think that such an attempt would overtax our present data base.

Figure 1. Comparison of momentum transfer dependence for E1 (MS model), E2 (GT) and E3 (GT) with $c_{tr}/c = 1.0$. The momentum transfer covered is indicated by the dashed vertical lines; it is sufficient to distinguish between E1, E2, and E3 excitations. To go to higher and lower momentum transfer would be desirable. To do so is ruled out at the present experimental situation because of the low duty factor (forward angles, low q) and low beam current (backward angle, high q).

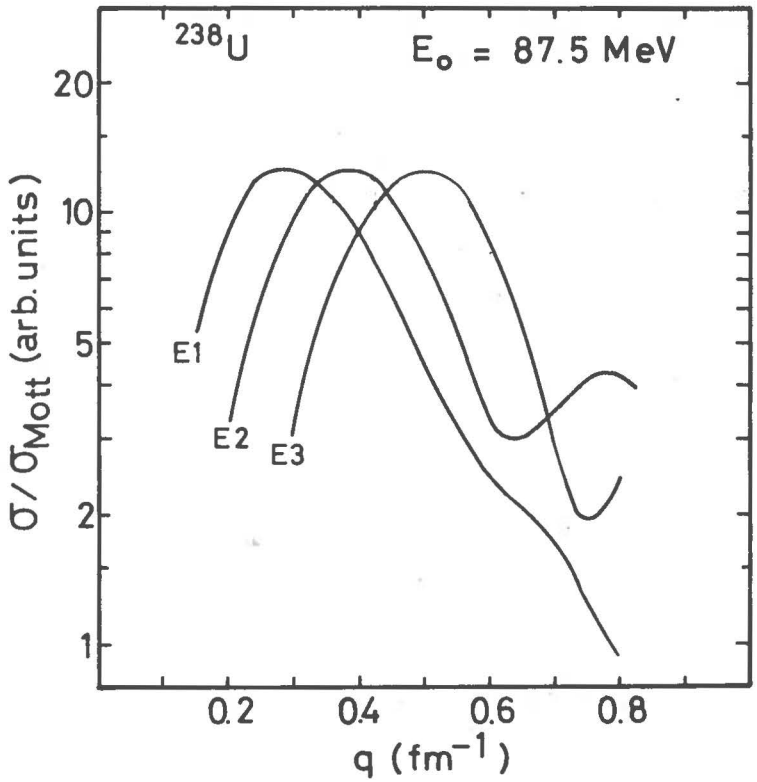

Figure 1

Figure 2. Spectrum of 87.5 MeV electrons scattered inelastically from ^{238}U at 75°. The total fitted background consisting of radiation tail, general room background, and experimental scattering is represented by the lowest heavy line.
The fitted resonances (lines between background and data points), and the composite fitted cross section (top line) are indicated. Note the suppressed scale; the resonant cross section is only a small fraction of the underlying radiation tail. The raising line at the very left is due to the tail of the ghost peak. The cross section has not been corrected for the constant dispersion of the magnetic spectrometer in order to show the data as measured. It is evident that not much can be learned from the data without background subtraction (see figure 3).

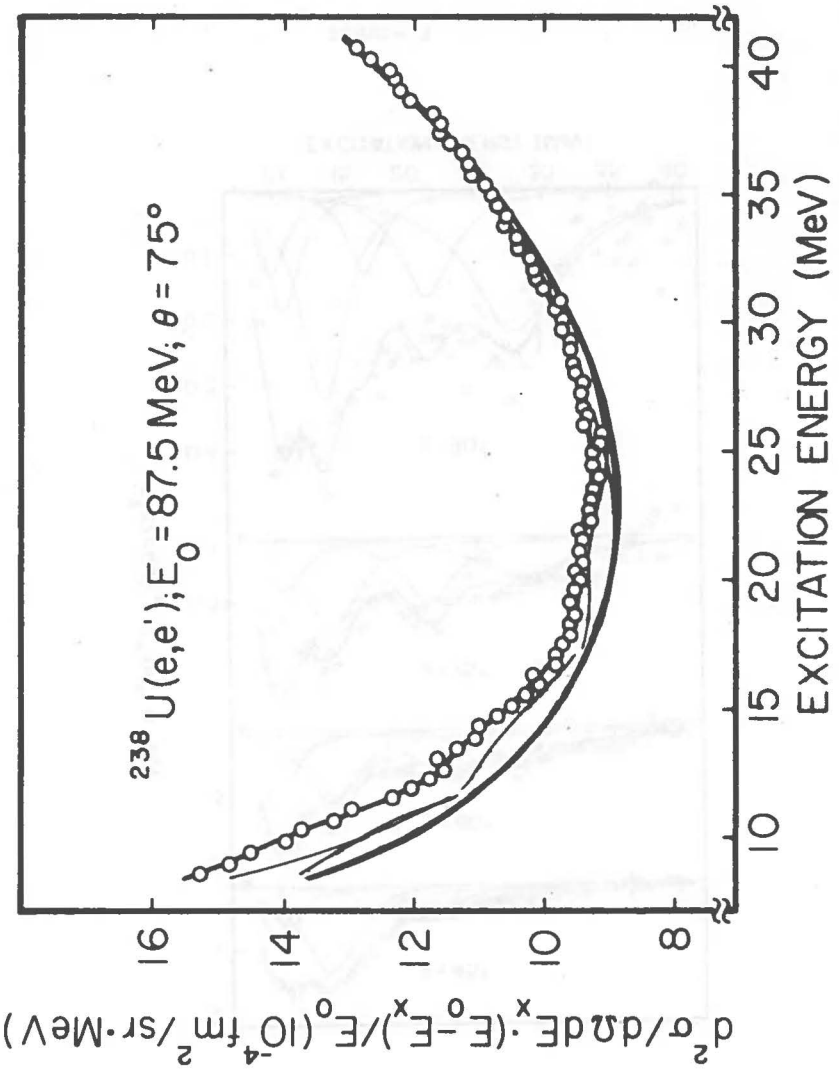

Figure 2

Figure 3. 87.5 MeV electrons scattered inelastically from ^{238}U at 45°, 60°, 75° and 90°. The fitted background, consisting of radiation tail, general room background and instrumental scattering, has been subtracted. Comparison of part c with figure 1 shows that after subtraction of background many more details show up. The data have been corrected for the constant dispersion of the magnetic spectrometer in order to show the cross sections of the various resonances in their true relation. The relative differences in peak height for different resonances at different angles show that several multipolarities contribute.

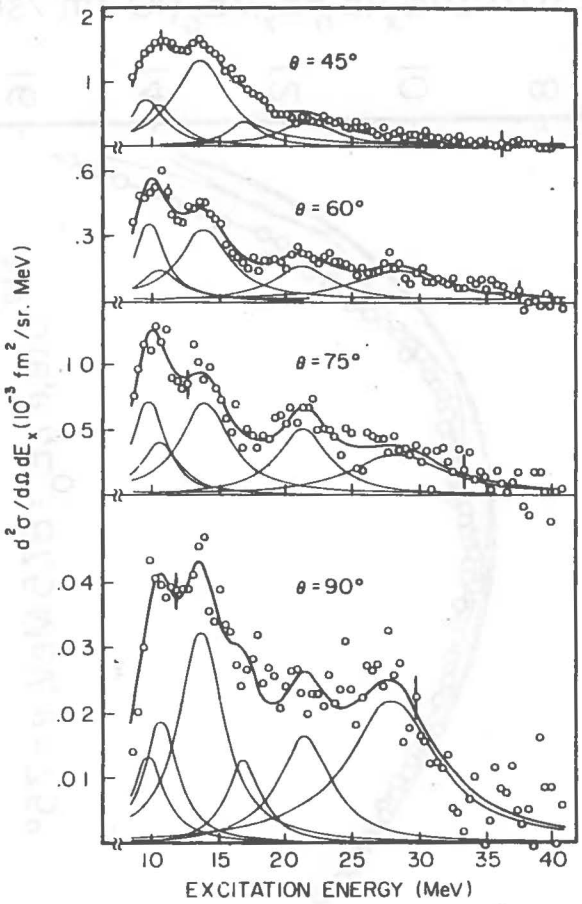

Figure 3

Figure 4. Strength of giant isoscalar quadrupole resonance as measured by (e,e') using a 'strict' (for definition see text) Goldhaber-Teller model. The result for ^{238}U is much lower than the value one would expect from any extrapolation of the data at lower A. The dashed line is for the guidance of the eye only and does not imply any theoretically or otherwise motivated fit to the data.

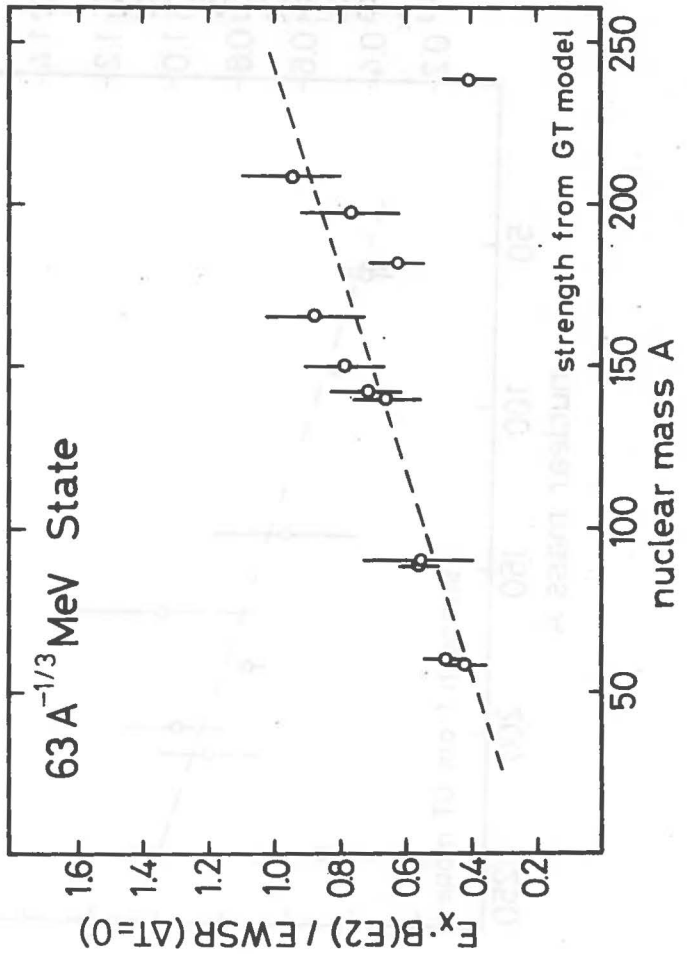

Figure 4

Figure 5. Similar to figure 4, but for the isovector GQR.

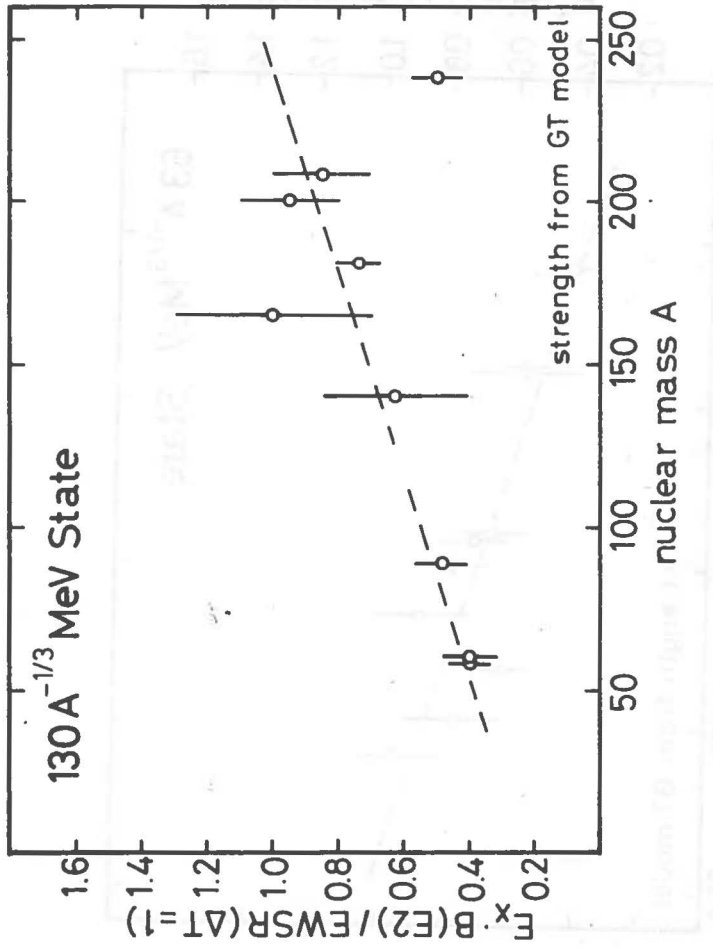

Figure 5

Figure 6. Model dependency study of the giant dipole resonance. DWBA calculations[42] for the Goldhaber-Teller[46,47], Steinwedel-Jensen[40,48] and Myers-Swiatecki[50] models are shown. The meaning of the parameterization[43] of the MS model is explained in the text. For GT and SJ model, an unmodified ground state charge distribution was assumed. From comparison of the transition radii (R_{tr}) connected with certain models and parameterizations it is clear that the behavior of the relative cross section σ/σ_{Mott} (formfactor) is determined by the value of R_{tr} alone up to approximately the first minimum or what is left of it in a heavy nucleus. The emphasis of the calculations was put on the MS model, because recent experiments[52] show it to describe the experimental data very well. The trend of the cross section to become smaller with larger R_{tr}'s is clearly visible, thus introducing a model dependency. The curves are normalized to unity in the reduced transition probability.

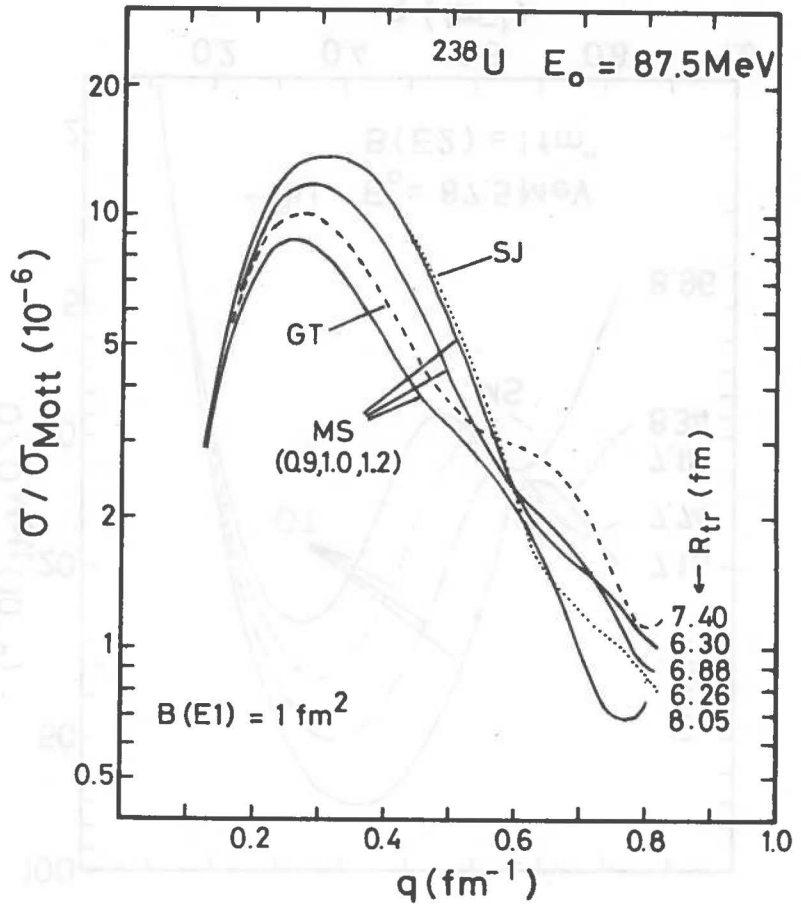

Figure 6

Figure 7. Similar to figure 6 but for an E2 transition. The emphasis here is on the GT model, because it is expected to describe the isoscalar excitation correctly[44]; a calculation with the MS model using $\alpha(238,2) = 1.0$ shows that similar to the dipole case R_{tr} determines the height of the curves, with the difference that, using the same parameterization as for figure 6, the differences for different para- are even more pronounced. The GT calculations correspond to parameter c_{tr}/c (ref. 43, see text) = 0.9, 1.0, 1.1 and 1.2, respectively, the MS model to $c_{tr}/c = 1.1$.

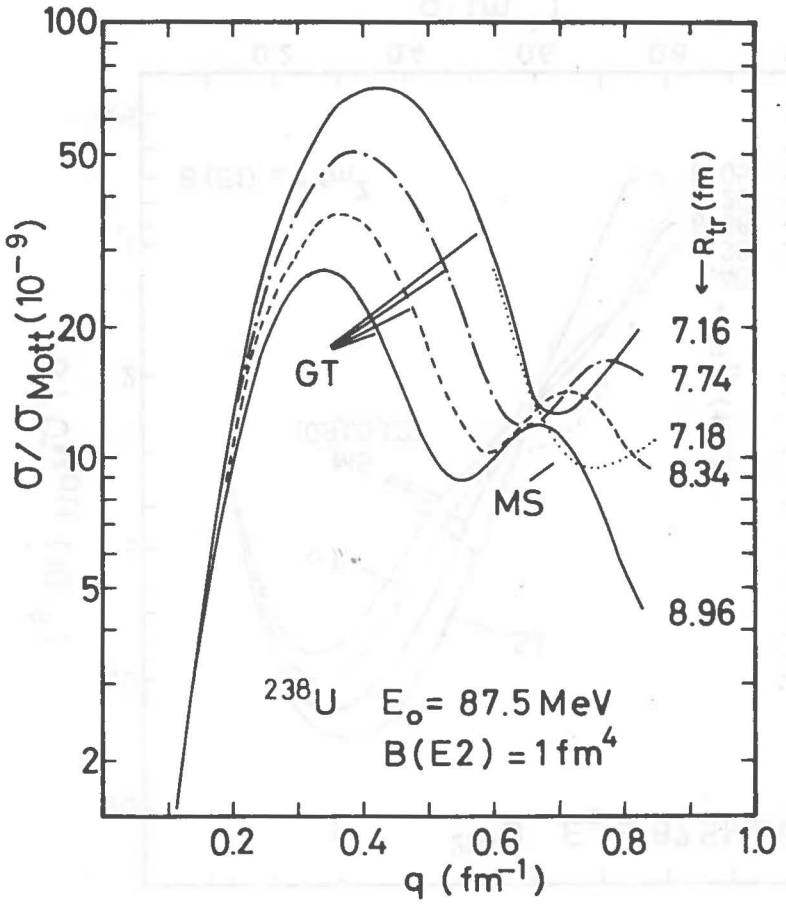

Figure 7

Figure 8. Similar to figure 6 and 7, but for an E3 transition. The trend to larger model dependencies with higher multipolarities, as already indicated by comparing figure 6 and 7, is continued. The four GT curves correspond to the same values in c_{tr}/c as in figure 7, the SJ curve to 1.1.

The MS curves similarly use a ground state charge distribution expanded by 10%, but vary in the additional parameter of the MS model, the mixture ratio α of SJ and GT mode. The higher MS curve thus corresponds to $\alpha = 1.0$, the lower to $\alpha = 0.5$.

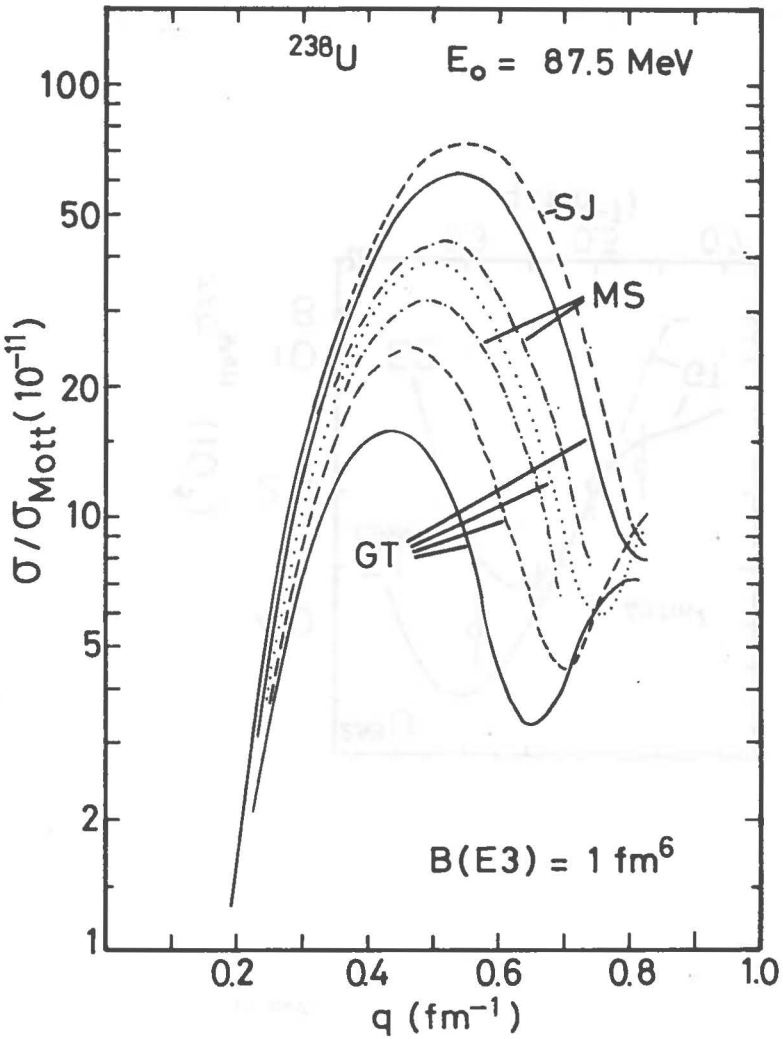

Figure 8

Figure 9. Comparison between experimental and DWBA (GT, $c_{tr}/c = 1$) formfactor for the GDR branch at 11 MeV (oscillation along long axis). The data are extremely well described by the calculation.

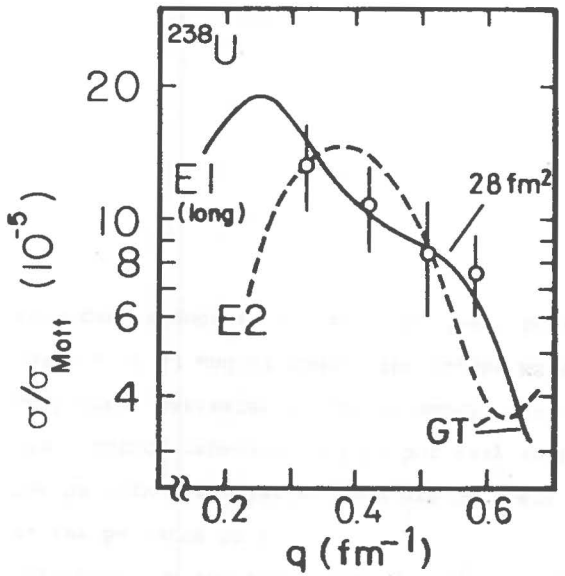

Figure 10. Similar to figure 9, but for the GDR resonance at 14 MeV.

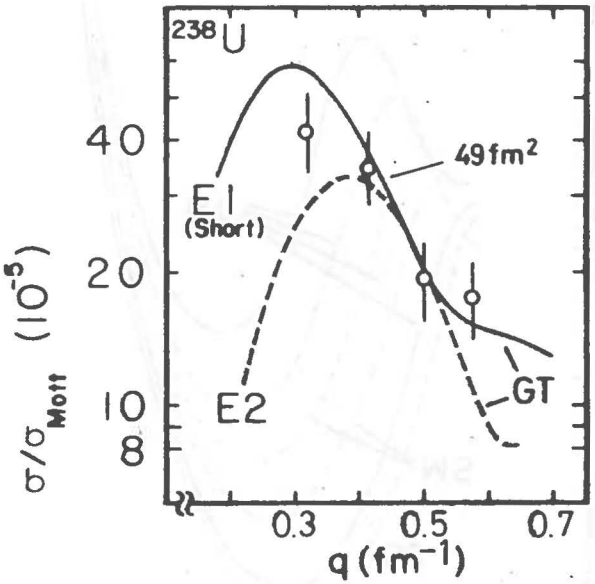

Figure 11. Comparison between MS model DWBA calculation, assuming a ground state charge distribution enlarged by 10% and the experimental data for both branches of the GDR. The resulting strength is close to the one extracted with the GT model in figures 9 and 10. On this basis no decision about the validity of either model and other underlying assumptions could be made (See text for more details).

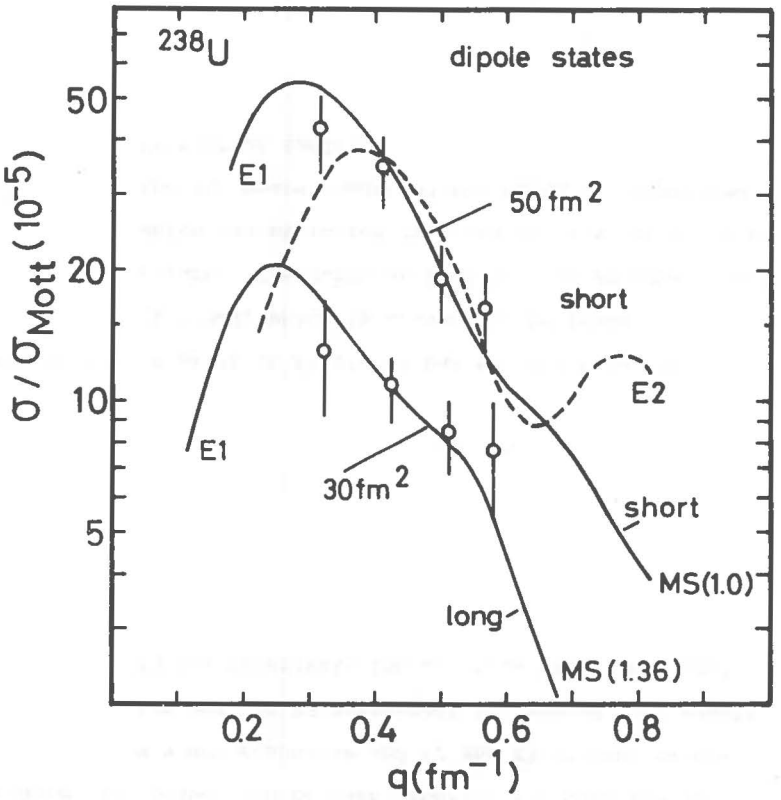

Figure 12. Comparison between experimental data for the 9.9 MeV resonance and E2 and E3 GT DWBA calculations. An E2 assignment is favored, but results in the relatively low sum rule value indicated

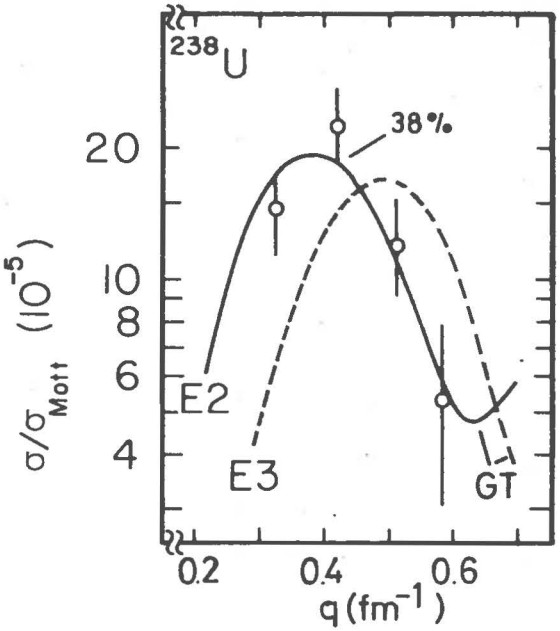

Figure 13. Similar to figure 12 but for the resonance at 21.6 MeV, which is assumed to be isovector in nature. The datum at 0.32 fm^{-1} is an upper limit which was estimated from the statistical error of the 45° measurement and the width as determined from other angles.

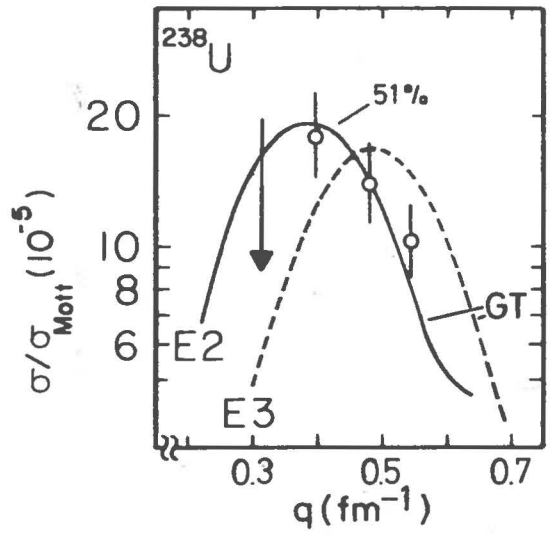

Figure 14. Comparison between the experimental data of figures 12 and 13 and DWBA calculations based on modified GT and MS models. If we follow the underlying hypothesis of this paper, namely the assumption of a spatially larger ^{238}U in the excited state as compared to the ground state, the data are well described by the DWBA calculations and are in agreement with other experiments and what we would expect from figures 4 and 5.

Figure 14

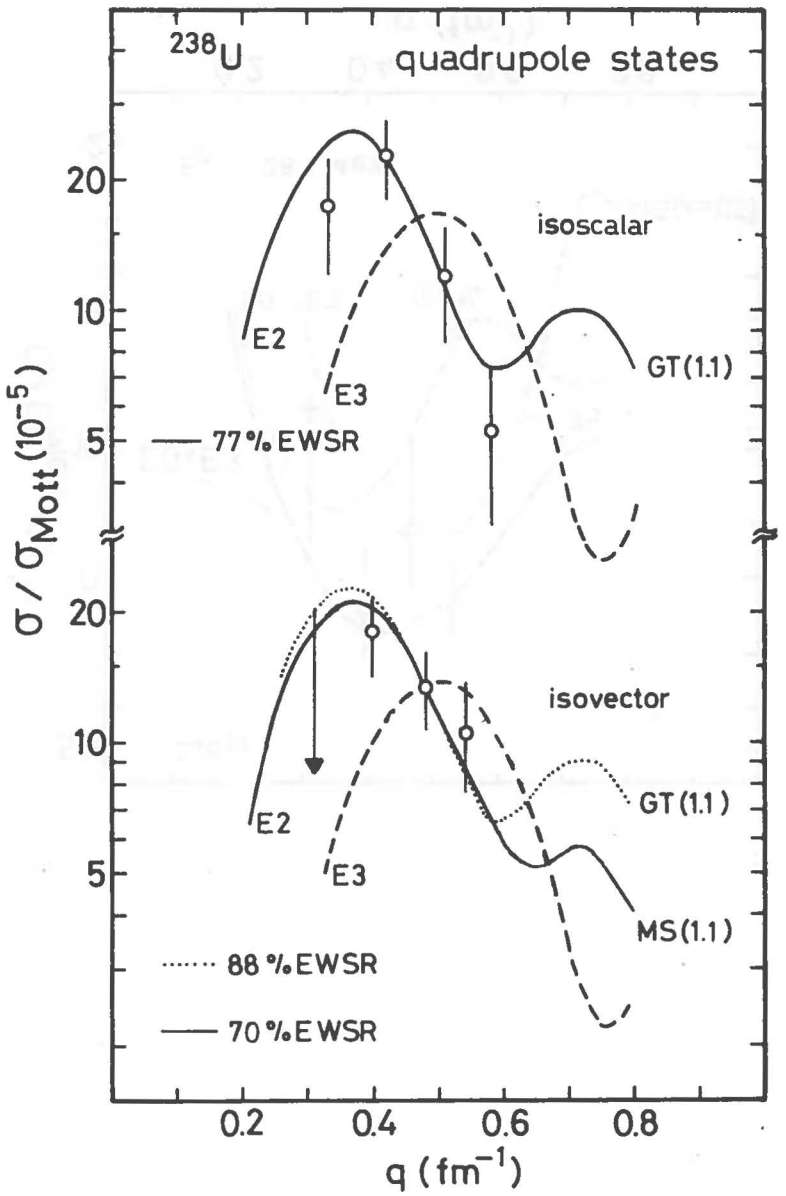

Figure 15. Comparison between the cross section of the 28.4 MeV resonance and DWBA calculations. Choosing $c_{tr}/c = 1.1$ in agreement with the parameterization for the other resonances is compatible with 100% of the isovector monopole plus 75% of the isovector octupole EWSR in this region. It should be emphasized, however, that assumption of exhausts 90% of the E3 EWSR on the basis of the GT model and fits the data nearly as well. Similar to figure 13 the upper limit at 0.30 fm^{-1} was estimated from the statistical error of the 45° data at 28.4 MeV and the width as determined from other angles. We think that the χ^2 fit would be sensitive to any larger cross section.

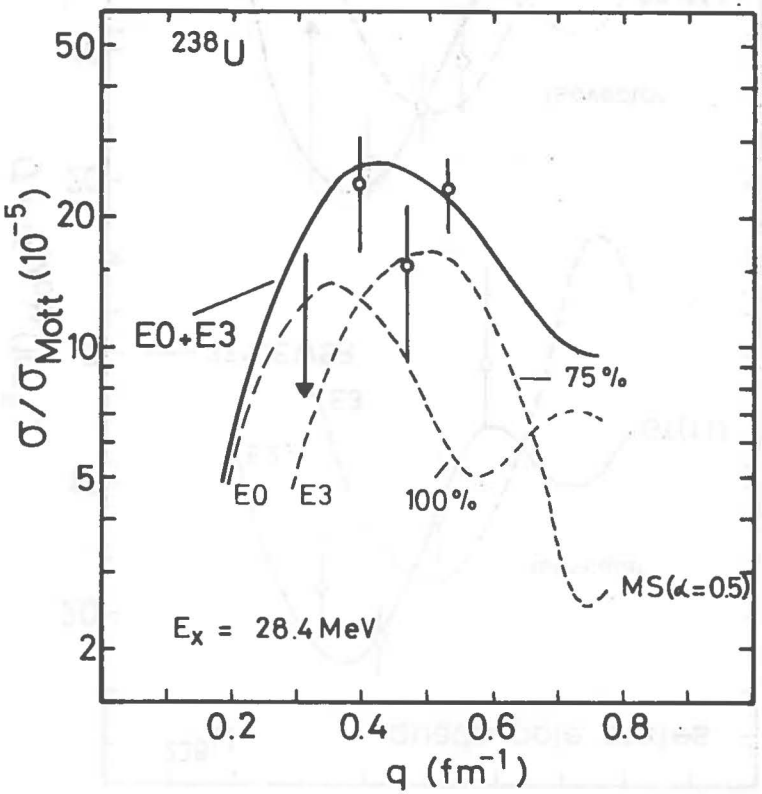

Figure 15

TABLE 1

	E1			E2			E3		
c_{tr}/c	R_{tr}^{GT}(fm)	R_{tr}^{MS} a) (fm)	R_{tr}^{SJ}(fm)	R_{tr}^{GT}(fm)	R_{tr}^{MS} b) (fm)	R_{tr}^{SJ}(fm)	R_{tr}^{GT}(fm)	R_{tr}^{MS} b) (fm)	R_{tr}^{SJ}(fm)
0.9	6.78	6.30	5.74	7.16	6.61	6.02	7.59		6.16
1.0	7.34	6.88	6.26	7.74	7.18	6.57	8.13		6.76
1.1	8.03	7.23	6.78	8.35	7.76	7.12	8.69	8.04	7.34
1.2	8.67	8.05	7.31	8.96	8.34	7.67	9.27	8.62	7.92
1.24	8.923								
1.36		8.99							

a) $\alpha = 0.9$

b) $\alpha = 1.0$

Transition radii $R_{tr} = \langle r^{\lambda+2} \rangle_{tr} / \langle r^2 \rangle_{tr}$ for various combinations of models, parameterizations, and multipolarities. This table is useful for a quantitative analysis of the model dependence as indicated by figures 4,5 and 6.

TABLE 2

Ref.	Reaction	E_x (MeV)	Long Axis Γ (MeV)	$B(fm^2)$	E_x (MeV)	Short Axis Γ (MeV)	$B(fm^2)$
20	(γ,n)	10.96 ± 0.09	2.90 ± 0.14	31	14.04 ± 0.13	4.53 ± 0.13	46
18	(γ,γ')	10.95 ± 0.06	2.62 ± 0.19	28	14.00 ± 0.68	4.53 ± 0.20	48
21	(γ,n)	10.80	2.44	28	13.85	5.12	65
19	(γ,n)	10.97 ± 0.13	2.99 ± 0.48	30	14.25 ± 0.18	5.10 ± 0.63	49
This work	(e,e')	10.75 ± 0.25	3.2 ± 0.4	28	13.95 ± 0.25	4.5 $^{+0.2}_{-0.3}$	49

Comparison of giant dipole resonance parameters from several experiments. The γ cross sections[18-21] have been converted into reduced transition probabilities using equation 9 of ref. 35. The other parameters, excitation energy and width, were not converted to those of the strength function, because for the E1 the resulting changes are relatively small[35], in any case smaller than the errors given. The strength given from this work is based on the 'strict' GT model; more detailed information can be found in the text and table 5.

Table 3

Nucleus	Γ_{exp} (MeV)	Γ_{theory} (MeV)	Ref. (exp)	Ref. (theory)
^{150}Nd	5.0 ± 0.2	5.0	12	39
^{154}Sm	4.7 ± 0.3	4.5	5	39
^{165}Ho	3.9 ± 0.4	3.9	13	a)
^{181}Ta	3.13 ± 0.55	—	45	—
^{238}U	5.1 ± 0.3 b)	2.9	28	39
	$2.9 \pm {}^{0.8}_{0.4}$		present work	39

a) S.V. Akulinichev and L.A. Malov, DUBNA preprint E4-9758, quoted in ref. 39.

b) Width of the strength function, that of the cross section as given in ref. 28 is 6.8 ± 0.4 MeV.

Comparison of the experimental spreading width of the isoscalar giant quadrupole resonance, in deformed nuclei resonance, as measured with (e,e'), (e,f), and (α,α'), with theoretical predictions based on Solovievs semi-microscopic model[39].

TABLE 4

Reference	E_x (MeV)	Γ (MeV)	R(%) a)	Reaction
22	10 - 13	—	85	(p,p')
28	9.9 ± 0.2	5.1 ± 0.3	71	(e,f)
This work	9.9 ± 0.2	$2.9 \pm {}^{0.8}_{0.4}$	77 b)	(e,e')

a) $R = E_x \cdot B(E2)/EWSR(E2,\Delta T = 0)$

b) Value based on a modified GT model with $c_{tr}/c = 1.1$

Comparison of available experimental results for the isoscalar quadrupole resonance.

TABLE 5

Summary of the quantitative results of this paper. While the excitation energy and the width of the resonant structures found is relatively insensitive to multipolarity and models used, the strength is not. For each resonance, two values are given. The upper value corresponds to a straight application of the GT model to the data. The lower value corresponds to the assumption of an ^{238}U nucleus which is spatially enlarged by approximately 10% as compared to the ground state. In addition, the MS model[50,51], was used for the isovector excitations. These assumptions lead to a greater consistency of the strength with other available data in lighter nuclei[8] and for ^{238}U.

TABLE 5

E_x (MeV)	Eλ	Model (c_{tr}/c)	$E_x(A^{-1/3}$MeV)	ΔT	Γ (MeV)	B(Eλ) ($fm^{2\lambda}$)	Γ_γ^o(eV)	SPU	R(%)[a]
9.9 ± 0.2	E2	GT(1.0)	62	0	$2.9^{+0.8}_{-0.4}$	3700	56	17	38 ± 10
		GT(1.1)				7500	114	35	77 ± 20
10.8 ± 0.3	E1	GT(1.24)	67	1	3.2 ± 0.4	28	$1.3\cdot10^4$	5	36 ± 4
		MS(1.35)[b]				30	$1.3\cdot10^4$	5	39 ± 4
13.9 ± 0.3	E1	GT(0.9)	86	1	$4.5^{+0.3}_{-0.4}$	49	$4.6\cdot10^4$	10	81 ± 8
		MS(1.0)[b]				50	$4.7\cdot10^4$	10	83 ± 8
21.6 ± 0.6	E2	GT(1.0)	133	1	5.0 ± 0.6	3600	$2.7\cdot10^3$	17	51 ± 8
		MS(1.1)[c]				5000	$3.7\cdot10^3$	23	70 ± 11
28.4 ± 1.2	E3	GT(1.0)	176	1	8.1 ± 1.1	$6.2\cdot10^5$	$5.4\cdot10^2$	78	91 ± 15
		MS(1.1)[d]				$5.1\cdot10^5$	$6.6\cdot10^2$	64	75 ± 12

a) $R = E_x \cdot B(E\lambda)/EWSR(E\lambda,\Delta T)$

b) $\alpha(238,1) = 0.9$

c) $\alpha(238,2) = 1.0$

d) $\alpha(238,3) = 0.5$

REFERENCES

1. B.R. Mottelson, in "Int. Conf. on Nucl. Structure", Kingston 1960, eds. D.A. Bromley and E.W. Vogt (Univ. of Toronto Press and North-Holland, Amsterdam, 1960); A. Bohr, in "Int. Nucl. Physics Conf.," Gatlinburg 1966, eds. R. Becker, C. Goodman, P. Stelson and A. Zucker (Academic Press, New York, 1967).
2. R. Pitthan and Th. Walcher, Phys. Lett. 36B, 563 (1971); Z. Naturforsch. 27a, 1683 (1972).
3. G.R. Satchler, Nucl. Phys. A195, 1 (1972).
4. S. Fukuda and Y. Torizuka, Phys. Rev. Lett. 29, 1109 (1972).
5. D.H. Youngblood, J.M. Moss, C.M. Rozsa, J.D. Bronson, A.D. Bacher and D.R. Brown, Phys. Rev. C13, 994 (1976).
6. J.M. Eisenberg and W. Greiner, "Nuclear Models", (North-Holland, Amsterdam, 1970).
7. A. Bohr and B.R. Mottelson, Nuclear Structure, Vol. 2 (Benjamin Reading, Mass., 1975).
8. R. Pitthan, Nukleonika 24 (1979), in press.
9. M. Danos, Nucl. Phys. 5, 264 (1958).
10. K. Okamoto, Phys. Rev. 110, 143 (1958).
11. Y. Torizuka, et al., in "Proc. Int. Conf. Nucl. Struct. Using Electron Scattering and Photoreaction", Sendai 1972, eds. K. Shoda and H. Ui, Suppl. Res. Report Lab. Nucl. Sci., Tohoku Univ., Vol. 5 (1972) p. 171.
12. A. Schwierczinski, R. Frey, E. Spamer, H. Theissen, and Th. Walcher, Phys. Lett. 55B, 171 (1975).
13. G.L. Moore, F.R. Buskirk, E.B. Dally, J.N. Dyer, X.K. Maruyama, and R. Pitthan, Z. Naturforsch. 31a, 668 (1976).
14. F.E. Bertrand, G.R. Satchler, D.J. Horen, and A. van der Wonde, Phys. Rev. C18, 2788 (1978).
15. T. Suzuki and D.J. Rowe, Nucl. Phys. A292, 93 (1977).
16. W.A. Houk, R.W. Moore, F.R. Buskirk, and R. Pitthan (unpublished), 1977.
17. T. Bar-Noy and R. Moreh, Nucl. Phys. A229, 417 (1974).
18. G.M. Gurevich, L.E. Lazareva, V.M. Mazur, and G.V. Solodukhov, JETP Lett. 20, 343 (1974) [ZhETF Pis. Red. 20, 741 (1974)].
19. G.M. Gurevich, L.E. Lazareva, V.M. Mazur, G.V. Solodukhov, and B.A. Tulupov, Nucl. Phys. A273, 326 (1976).
20. A. Veyssière, H. Beil, R. Bergère, P. Carlos, A. Leprêtre, and K. Kernbath, Nucl. Phys. A199, 45 (1973).
21. J.T. Caldwell, E.J. Dowdy, B.L. Berman, R.A. Alvarez, P. Meyer, Los Alamos Scientific Laboratory Report LA-UR76-1615, quoted in Lawrence Livermore Laboratory Report UCRL-78482, Atlas of Photoneutron Cross Sections Obtained with Monoenergetic Photons, ed. B.L. Berman.
22. M.B. Lewis and D.J. Horen, Phys. Rev. C10, 1099 (1974).
23. E. Wolynec, M.N. Martins, and G. Moscati, Phys. Rev. Lett. 37, 585 (1976).
24. J.C. McGeorge, A. Shotter, C. Zimmerman and A. Flowers, J. Phys. G.: Nucl. Phys. 4, L145 (1978); D.H. Dowell, P. Axel, and L.S. Cardman, Phys. Rev. C18, 1550 (1978).
25. W.R. Dodge, E. Hayward, G. Moscati, and E. Wolynec, Phys. Rev. C18, 2435 (1978).
26. A.C. Shotter, J.M. Reid, J.M. Hendry, D. Branford, J.C. McGeorge, and J.S. Barton, J. Phys. G.: Nucl. Phys. 2, 769 (1976).
27. U. Kneissl, G. Kuhl, K.H. Leister, and A. Weller, Nucl. Phys. A256, 11 (1976).

28. J.D.T. Arruda Neto, S.B. Herdade, B.S. Bhandari, and I.C. Nascimento, Phys. Rev. C18, 863 (1978).

29. R. Pitthan, F.R. Buskirk, E.B. Dally, J.O. Shannon, and W.H. Smith, Phys. Rev. C16, 970 (1977).

30. R. Pitthan, H. Hass, D.H. Meyer, F.R. Buskirk, and J.N. Dyer, Phys. Rev. C19, (1979); in press.

31. R. Pitthan, F.R. Buskirk, E.B. Dally, J.N. Dyer and X.K. Maruyama, Phys. Rev. Lett. 33, 849 (1974); 34, 848 (1975).

32. C.R. Fischer and G.H. Rawitscher, Phys. Rev. 135B, 377 (1964).

33. C.W. de Jager, H. de Vries and C. de Vries, Atomic Data and Nuclear Data Tables 14, 479 (1974).

34. E.S. Ginsberg and R.H. Pratt, Phys. Rev. 134B, 849 (1964).

35. E.F. Gordon and R. Pitthan, Nucl. Instrum. Methods 145, 569 (1977).

36. E.C. Halbert, J.B. McGrory, G.R. Satchler, and J. Speth, Nucl. Phys. A245, 189 (1975).

37. O. Nathan and S.G. Nilsson, in "Alpha, Beta, and Gamma Spectroscopy", ed. K. Siegbahn (North-Holland, Amsterdam, 1965).

38. J. Weneser and E.K. Warburton, in "The Role of Isospin in Nuclear Physics", ed. D.H. Wilkinson (North-Holland, Amsterdam 1969).

39. G. Kyrchev, L.A. Malov, V.O. Nesterenko, and V.G. Soloviev, Sov. J. Nucl. Phys. 25, 506 (1977) [Yad. Fiz. 25, 951 (1977)].

40. A. Migdal, J. Phys. USSR 8, 331 (1944); J.S. Levinger, "Nuclear Photodisintegration", (Oxford University Press, New York, 1960).

41. R.A. Ferrell, Phys. Rev. 107, 1631 (1957).

42. S.T. Tuan, L.E. Wright, and D.S. Onley, Nucl. Instrum. Methods 60, 70 (1968).

43. J.F. Ziegler and G.A. Peterson, Phys. Rev. 165, 1337 (1968).

44. T.J. Deal and S. Fallieros, Phys. Rev. C7, 1709 (1973).

45. R.S. Hicks, I.P. Auer, J.C. Bergstrom and H.S. Caplan, Nucl. Phys. A278, 261 (1977).

46. L.J. Tassie, Austral. J. Phys. 9, 407 (1956).

47. M. Goldhaber and E. Teller, Phys. Rev. 74, 1046 (1948).

48. H. Steinwedel and H. Jensen, Z. Naturforsch. 5a, 413 (1950).

49. W.D. Myers and W.J. Swiatecki, Ann. Phys. (N.Y.) 55, 395 (1969).

50. W.D. Myers, W.J. Swiatecki, T. Kodama, L.J. El-Jaick, and E.R. Hilf, Phys. Rev. C15, 2032 (1977).

51. T. Kodama (unpublished, 1978).

52. R. Pitthan, H. Hass, D.H. Meyer, J.N. Dyer, and F.R. Buskirk, Phys. Rev. Lett. 41, 1276 (1978).

53. F.E. Bertrand, Ann. Rev. Nucl. Sci. 26, 457 (1976).

54. T. Kishimoto, J.M. Moss, D.H. Youngblood, J.D. Bronson, C.M. Rosza, D.R. Brown, and A.D. Bacher, Phys. Rev. Lett. 35, 552 (1975).

55. D.H. Youngblood, C.M. Rosza, J.M. Moss, D.R. Brown, and J.D. Bronson, Phys. Rev. Lett. 39, 1188 (1977).

56. D. Zawischa and J. Speth, Phys. Rev. Lett. 36, 843 (1976).

57. N. Auerbach and A. Yeverechyahu, Ann. Phys. (N.Y.) 95, 35 (1975).

58. N. Auerbach and A. Yeverechyahu, Phys. Lett. 62B, 143 (1975).

59. T. Suzuki and D.J. Rowe, Nucl. Phys. A292, 93 (1977).

60. S.V. Akulinichev and L.A. Malov, J. Phys. G.: Nucl. Phys. 3, 625 (1977).

61. V.G. Soloviev, Report at the 28th Symposium on Nuclear Spectroscopy and Nuclear Structure, Alma Ata, 1978 (to be published in Isvestia Akademia Nauk USSR (Ser. Fiz.)).

62. I. Hamamoto, ref. 11, p. 208.

63. T. Suzuki, Nucl. Phys. A217, 182 (1973).

64. K.F. Liu and G.E. Brown, Nucl. Phys. A265, 385 (1976).

65. Th. H. Schucan, Nucl. Phys. 61, 417 (1965).

66. G.R. Satchler, Part. Nucl. 5, 105 (1973).

26a. A.C. Shotter, D. Branford, J.C. McGeorge, and J.M. Reid, Nucl. Phys. A290, 55 (1977).

26b. A.C. Shotter, C.H. Zimmerman, J.M. Reid, J.C. McGeorge, and A.G. Flowers, to be published in Nucl. Physics.

DEPARTMENT OF THE NAVY
Naval Postgraduate School
Monterey, California 93940

OFFICIAL BUSINESS
Penalty For Private Use $300

POSTAGE AND FEES PAID
DEPARTMENT OF THE NAVY
DOD - 316

DR.XAVIER K. MARUYAMA
NAT.BUR.STANDARDS
CENTRE F.RAD.RES.
WASHINGTON DC 20234